ANALYTICAL STUDIES ON A 6-STORY FULL-SCALE REINFORCED CONCRETE WALL-FRAME STRUCTURE TO COLLAPSE

Y. Kim[1], T. Kabeyasawa[2], T. Matsumori[3] and T. Kabeyasawa[4]

[1] *Assistant Professor, Earthquake Research Institute, University of Tokyo, Tokyo, Japan*
[2] *Professor, Earthquake Research Institute, University of Tokyo, Tokyo, Japan*
[3] *Researcher, National Research Institute for Earth Science and Disaster Prevention, Hyogo, Japan*
[4] *Researcher, Structural Engineering Research Center, Tokyo Institute of Technology, Tokyo, Japan*
Email: yskim@eri.u-tokyo.ac.jp

ABSTRACT:

A 6-story full-scale reinforced concrete building subjected to severe earthquake loading simulated by E-Defense at Kobe, Japan experienced the collapse process which was planned and expected in preliminary analysis. In this paper, in addition to the brief description about experiment, modified modeling approaches on the evaluation of stiffness, strength and support condition of specimen are introduced to improve the quantitative correlation (e.g. displacement and base shear) between test and analysis. The reevaluation of initial stiffness resulting skeleton curve to be modified gave a good agreement between test and analysis and the increased girder strength enhanced the shear force carried by columns, leading maximum base shear to be reproduced in analysis.

KEYWORDS: full-scale shake table test, reinforced concrete, collapse, effective slab width

1. INTRODUCTION

With the aim of simulating the actual seismic behavior of reinforced concrete structure, a shake table test on a 6-story full-scale RC building structure was carried out at E-Defense of NIED in January 2006. The full-scale specimen comprises an open frame, a shear wall fame and a spandrel beam frame with short columns in longitudinal direction, which generate moderate uni-axial eccentricity in plan. As expected from the preliminary analyses, shear failures of short columns and shear wall in the 1st story induced the specimen to collapse under simultaneous 3-dimensional earthquake loadings.

Previous analytical studies (Kim 2005 and Kim 2007) incorporating strength degrading models into the shear critical members such as short column and shear wall had provided satisfying reproduction of the post peak behaviors characterized by strength deterioration leading shear force redistribution to the adjacent frames and displacement concentration on the 1st story. However, the quantitative comparison between test and analysis had shown substantial discrepancies in the maximum displacement and base shear.

In current analytical study, modified modeling approaches on the evaluation of stiffness, strength and support condition of specimen are adopted to improve the quantitative correlation between test and analysis throughout all damage stages. Instead of applying strength deteriorating model to short columns and shear wall, conventional analytical member models whose hysteretic behavior is not capable of representing strength softening in post-peak region are employed. Accordingly, observed large displacement at the first story resulting from strength degradation cannot be simulated in this analysis, and reproducing base shear versus displacement response in post-peak range is beyond the scope of this study. This study focused on evaluating shear force distribution carried by each frame and reproducing maximum base shear which had been underestimated from previous analytical works.

2. SHAKE TABLE TEST AT E-DEFENSE

The shake table test on a full-scale reinforced concrete structure (Figure 1) designed in accordance with 1970's design practice in Japan was performed at E-Defense, a 3-Dimensional earthquake simulator, in January 2006. It is six-story high and 2x3 bay in plan. The height of each story is 2.5m and the span length is 5m, which result in 15m in total height and 10x15m in plan, respectively. The structural weight of the specimen above top of foundation girder is about 7.5MN and the total weight of test structure mounted on the shake table is about 10MN that almost reach the maximum payload of E-Defense, 12MN. Longitudinal direction in plan (Y-direction) comprises three different kinds of frames such as a spandrel beam frame with short columns (X1 frame), a shear wall frame (X2 frame) and an open frame (X3 frame). As a result, different stiffness and strength between X1 and X3 frame generate uni-axial (Y-axis) stiffness and strength eccentricity. And the transverse direction (X-direction) with symmetric plan consists of two open frames and two wing wall frames providing X direction with relatively high strength and stiffness that resist against the torsional response induced from eccentricity in Y- axis. As input ground motions, three components (EW, NS and UD) of Kobe earthquake (JMA, 1995) are applied to the specimen simultaneously. North-south (NS) and east-west (EW) components are loaded to the specimen with an angle of 45 degree and 135 degree rotated from the X-axis, respectively, so that the earthquake input direction to the specimen is concentrated on Y-direction. Table 1 illustrates the loading sequence and maximum accelerations recorded from shake table that showed slightly lager maximum acceleration compared to the target acceleration. During INPUT-5, short columns in X1-frame and a shear wall in X2 frame failed in shear, which lead the specimen to collapse. Further information about experimental setup and results are available in Matsumori 2006 and Shirai 2006.

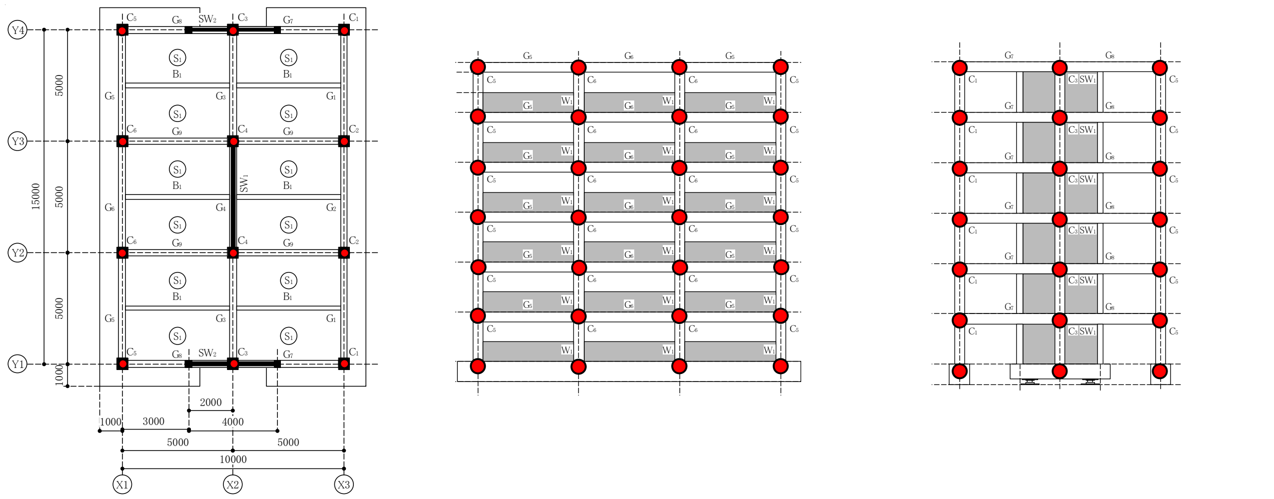

(a) Plan (b) Spandrel beam frame (X1) (c) Wing wall frame (Y1, Y4)

Figure 1 Full-scale specimen

Table 1. Loading sequence and recorded base motion from shake table

Input No.	Earthquake data	Scale factor	Maximum acceleration, m/s/s		
			X	Y	Z
INPUT-1	Kobe (JMA, 1995)	5%	0.307	0.469	0.191
INPUT-2		10%	0.785	0.916	0.391
INPUT-3		25%	1.97	2.99	0.946
INPUT-4		50%	3.43	4.74	1.86
INPUT-5		100%	6.30	11.40	3.45
INPUT-6		60%	3.11	5.40	1.93

3. ANALYSIS METHODOLOGY

3.1. Node

Figure 1 shows the nodal coordinates in plan and elevation of a specimen, which locate at the joint of girder and column. Each node has six-degree of freedoms, which are 3-translational and 3-rotational components. Since the floor is assumed as a rigid diaphragm in current analytical study, the translational behaviors in X and Y direction and rotational behavior in Z–axis in the same floor are coupled with each other. 1.2MN per floor is divided by a tributary area and lumped to each node and gravity load calculated from these nodal weights was taken into account as an initial axial load for vertical members.

3.2 Member Model

All columns and girders are idealized by line element model with 2-node and only shear wall is modeled by plate element model with 4-node. Although waist wall in X1 frame and wing wall in Y1 and Y4 frame are plate members, they are also modeled by line element model linked with just two end nodes (Figure 1 (b), (c)). The height of a waist wall and the width of a wing wall are modeled by rigid zone of side columns and boundary beams and are taken into account in calculating stiffness and strength of spandrel beam and wing wall as shown in Figure 2, respectively. And the effective slab width is also evaluated in girder section. Rigid diaphragm for slab in its own plane and rigid beam-column joints are assumed throughout this analytical study.

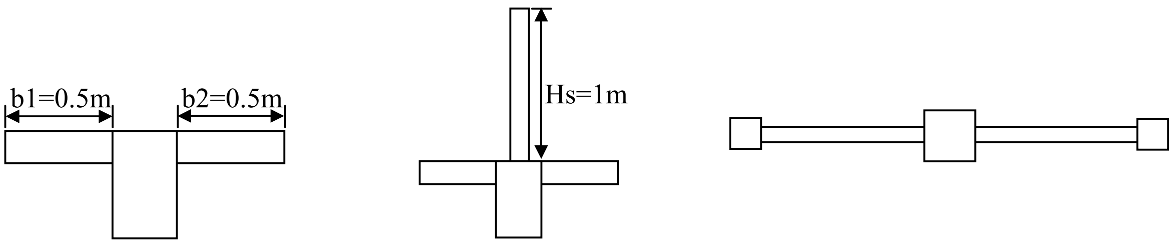

(a) T-shaped girder (b) Spandrel beam (X1 frame) (c) Wing wall (Y1 and Y4 frame)

Figure 2 Member sections

Flexural behaviors of all members are represented by lumped plastic hinge model, and axial behavior of column and shear wall are modeled by axial spring. The axial deformation of girder is not allowed because of rigid diaphragm assumption. Three-vertical-line element model is employed (Figure 3(a)) to model the shear wall in X2-frame. All hysteretic behavior of rotational spring and shear spring are represented by Takeda model, and axial spring is modeled by axial stiffness model as shown in Figure 3 (b) and (c).

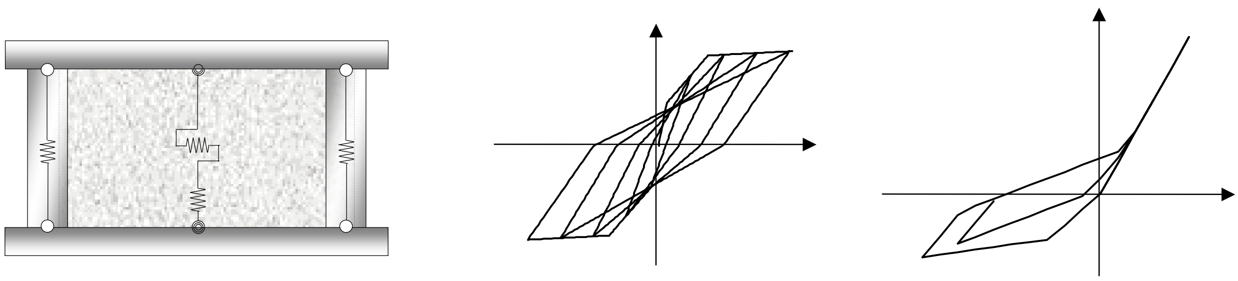

(a) Three vertical line element model (b) Takeda model (c) Axial stiffness model

Figure 3 Three vertical line element model and hysteretic model

3.3. Member strength

To take into account the dynamic loading effects on member strength, compressive strength of concrete and yield strength of steel obtained from cylinder and coupon test are scaled by factor 1.2. Although strain rate of steel and concrete is not confirmed in this shake table test, previous research of dynamic loading effects on strength enhancement has shown that the strength of members subjected to dynamic loading ranged between 1.1 and 1.5 times to those of statically loaded members. By using the scaled material properties, flexural strength and shear strength of members are calculated based on the equations in AIJ 1999. Specially, flexural strengths of spandrel beam and wing wall are calculated following the equations in The Japan Building Disaster Prevention Association 2001.

3.4 Support condition

Besides the structural members described above, support condition of a specimen is modeled by vertical and horizontal springs, which represent three directional load cells installed to measure shear force and axial force of shear wall and wing walls as shown in Figure 4. Horizontal and vertical stiffness of a load cell unit comprised of 4 load cells are 50MN/mm and 70MN/mm, respectively, which were obtained from loading test on a load-cell before attaching it to the specimen. In spite of high stiffness that is unlikely to allow deformation in load cell under current earthquake loading, foundation deformation was observed throughout all input stages. Those deformations were developed at bolt connection between steel plate and load cell (Figure 4) and sliding between foundation and shake table was observed at INPUT-5. Therefore, the stiffness of support spring representing four-load cell units (e.g. 16 load cells, Figure 4) is recalculated from the observed relationship between base shear and foundation deformation at INPUT-3 and INPUT-4 loading stage.

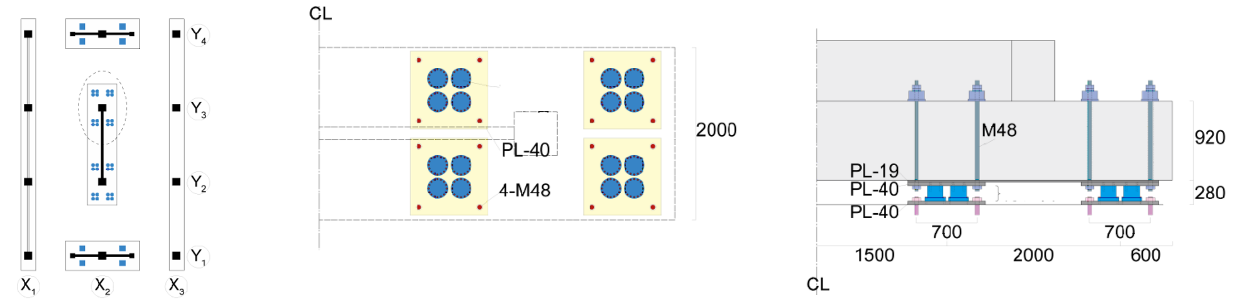

(a) Basement plan (b) Plan of X2-Y3 foundation (c) Elevation of X2-Y3 foundation

Figure 4 Installation of load cell

3.5 Analytical method

Among the six earthquake loadings (Table 1), INPUT-3, 4 and 5 are adopted in this analysis. For the purpose of considering the stiffness degradation and the residual displacement, three earthquake loadings (25%, 50% and 100%) were consecutively applied to the specimen. Three translational and three rotational accelerations recorded from the shake table were applied to the specimen in current analytical study. The Newmark-β method (β=0.25) was used to integrate the equation of motion in the time-history analyses and the integration time-step was equal to 0.01 second. The damping matrix is assumed to be proportional to the instant stiffness matrix and 3% of damping ratio was used throughout analyses.

4. ANALYTICAL RESULTS

Since the member models employed in this analytical study are not capable of simulating the strength deterioration inducing displacement concentration, current analytical model is not expected to reproduce the large displacement in post-peak region during INPUT-5. Therefore, only the analytical result until the maximum base shear is recorded is compared with experimental results. And in this chapter, two analytical results are shown, one of which is obtained from the model (CASE 1) described previous chapter and the other one is the model (CASE 2) modified from the CASE 1.

4.1 CASE 1: Proto-type

Figure 5 shows the relationship between base shear and 2nd floor drift ratio in X and Y direction of three input stages (i.e. INPUT-3, INPUT-4 and INPUT-5). Calculated stiffness is larger than that of observed results, and therefore displacements are underestimated in analysis. Base shear are also underestimated in analysis throughout all input stages. Observed maximum base shear during INPUT-5 is 7.41MN among which shear force carried by shear wall in X2-frame is 3.58MN. In analytical results until 6.78 second at which maximum base shear was recorded in test, calculated maximum base shear is 6.7MN, and the shear force resisted by shear wall is 3.57MN. This result shows that the shear force carried by shear wall in analysis is almost equivalent to observed results but the shear force carried by columns (3.13MN) is much smaller than that of test (3.83MN). The large fraction of difference in maximum base shear between test and analysis arose from the shear force carried by columns.

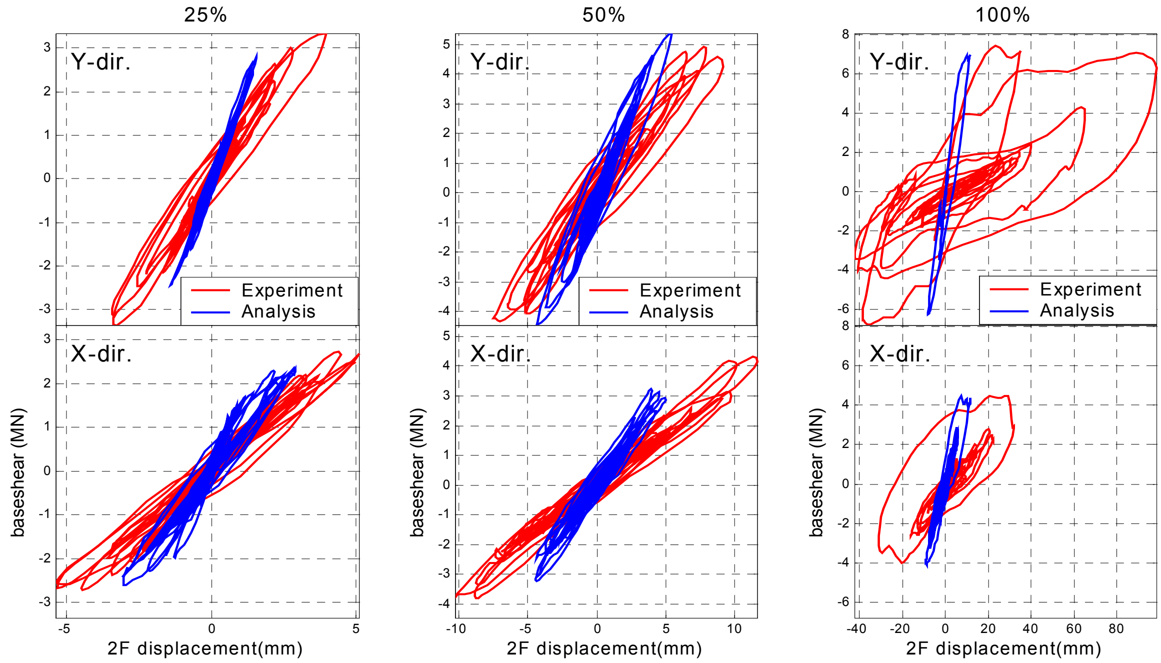

Figure 5 Relationship between base shear and 2F displacement (CASE1)

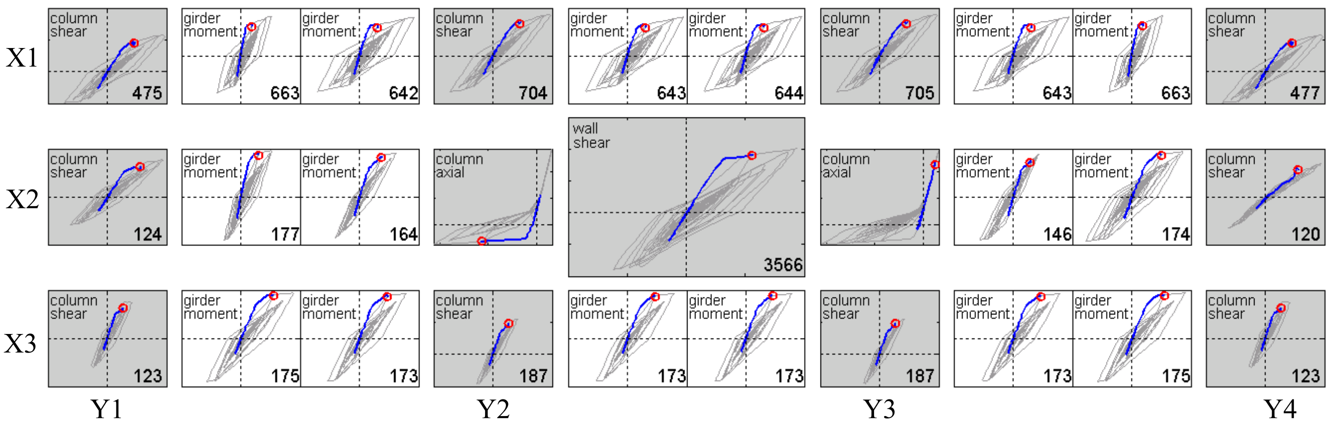

Figure 6 Response of members in the 1st story (unit: column and wall shear (kN), girder moment ($kN \cdot m$))

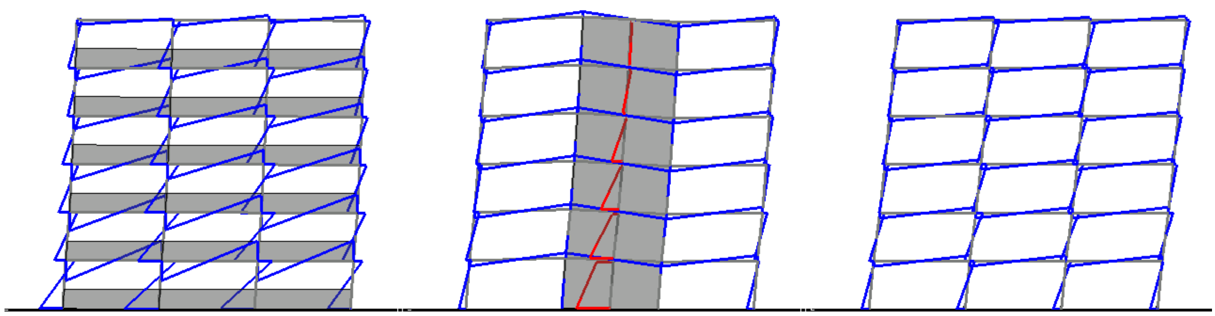

(a) X1 frame (b) X2 frame (c) X3 frame

Figure 7 Moment diagram in Y-direction

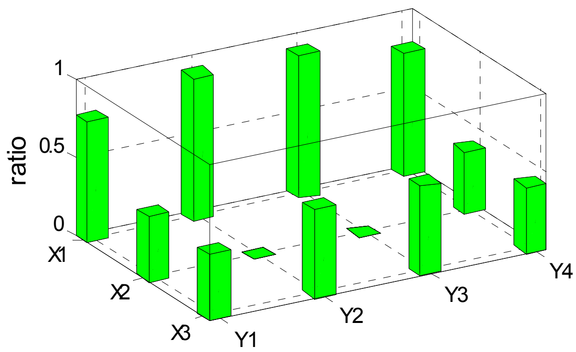

Figure 8 Ratio of shear force to shear strength of column at flexural yielding

For the purpose of investigating the shear force carried by each frame, the responses of each member in the first story are shown in Figure 6, where the thick line indicates the response until 6.78sec (circle marker) and numbers indicates the shear force (kN) of column and shear wall and bending moment ($kN \cdot m$) of girder. The shear force of column was calculated from the summation of two end moments divided by clear height of column. From this figure, it can be seen that the shear force carried by short columns in X-1 frame is almost three times to that of the other columns.

In addition to Figure 6, the moment diagram shown in Figure 7 also indicates that all the short columns in X1 frame have yielded at bottom and plastic deformation exceeding yield point has been developed when the maximum base shear was recorded, but the columns in X2 and X3 frame have not yielded or just yielded at bottom. Figure 7 also shows that the contra-flexural point of short columns at the 1st story is closer to the mid height of column than those of columns in X2 and X3 frame, which might cause the underutilization of shear capacity of column in X2 and X3 frame.

The sum of shear strength (at flexural yielding) of the first story columns is about 4.58MN, in which the side columns attached to the shear wall (X2Y2 and X2Y3) are not included. Figure 8 indicating the ratio of shear force carried by columns to the shear strength of column at flexural yielding illustrates that the shear force carried by the columns in X2 and X3 frame is only a half of their shear capacity.

It is interesting to note that all girders, as though the lateral load carrying capacity of columns was not fully exerted, have yielded (Figure). From these results, it can be stated that the girder strength in current analysis is underestimated and therefore the increased girder strength may enhance the utilization of column shear capacity.

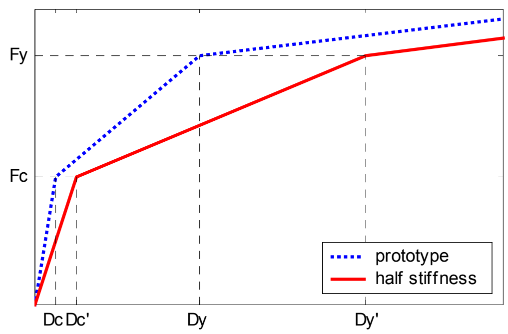

Figure 9 Skeleton curve

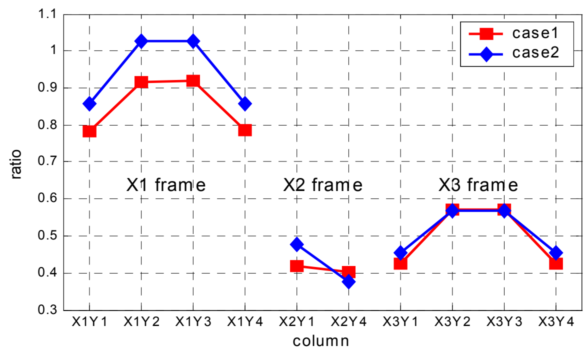

Figure 10 Ratio of column shear force to shear strength at flexural yielding

4.2 CASE 2: Modified initial stiffness and girder strength

From the comparison between test and analysis in previous section, it is shown that the displacement and the shear force carried by columns were underestimated in CASE 1 model. In this section, the analytical model of full-scale specimen was modified to improve the correlation between test and analysis. Initial stiffness of all members is reduced to half of the prototype model (i.e. CASE 1), which shows good agreement between test and analysis results in INPUT-3 where the specimen showed almost elastic behavior. Figure 9 illustrates the modified skeleton curve after initial stiffness is reduced to half of the prototype model, from which it can be seen that not only initial stiffness but also stiffness after crack is reduced. Increased crack and yield deformation in modified backbone curve (Figure 9) might be resulted from the additional deformation factors; e.g. pull-out response, beam column joint deformation, shear deformation and so on which are not taken into account in current model.

The flexural strength of girder is reevaluated by increasing the effective slab width. Increased strength of girder may enhance the shear force carried by column, which was underestimated in CASE 1 model. The effective slab widths of girders (b1 and b2 in Figure 2) along the perimeter (X1, X3, Y1 and Y4 frame) are set to 100cm and 200cm and those of the other girders (X2, Y2 and Y3 frame) linked to shear wall are set to 200cm and 200cm, respectively. Here, 100cm is maximum slab width attached to the outside of perimeter frame (Figure 1).

Figure 10 compares the ratio of column shear force to shear strength at flexural yielding between CASE 1 and CASE 2 model. By increasing the girder strength, the shear force carried by short columns in X1 frame is increased compared to the other columns in X2 and X3 frame. This shear force distribution between frames shows that short columns in X1 frame played an important role in resisting lateral load, which can be verified form the observed wide crack in short column (X1Y2) when the maximum base shear was recorded in test. Form the reevaluation in initial stiffness and girder strength, base shear and shear force carried by columns until 6.78 second could be reproduced in modified model (CASE 2) as shown in Figure 11.

Photo 1. Crack in short column at Max. base shear

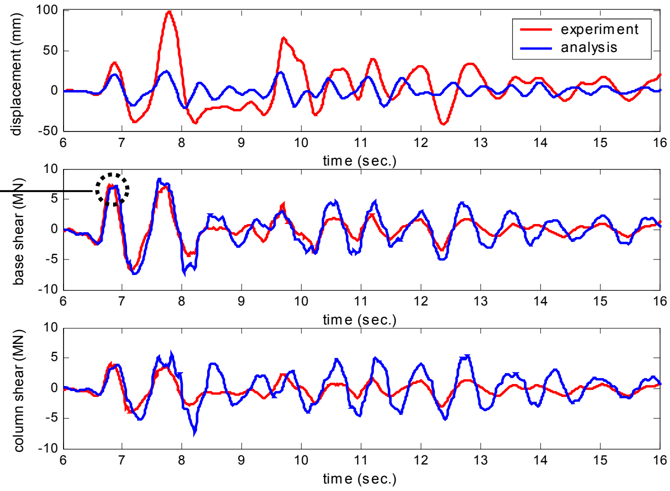

Figure 11 Displacement and shear force during INPUT-5

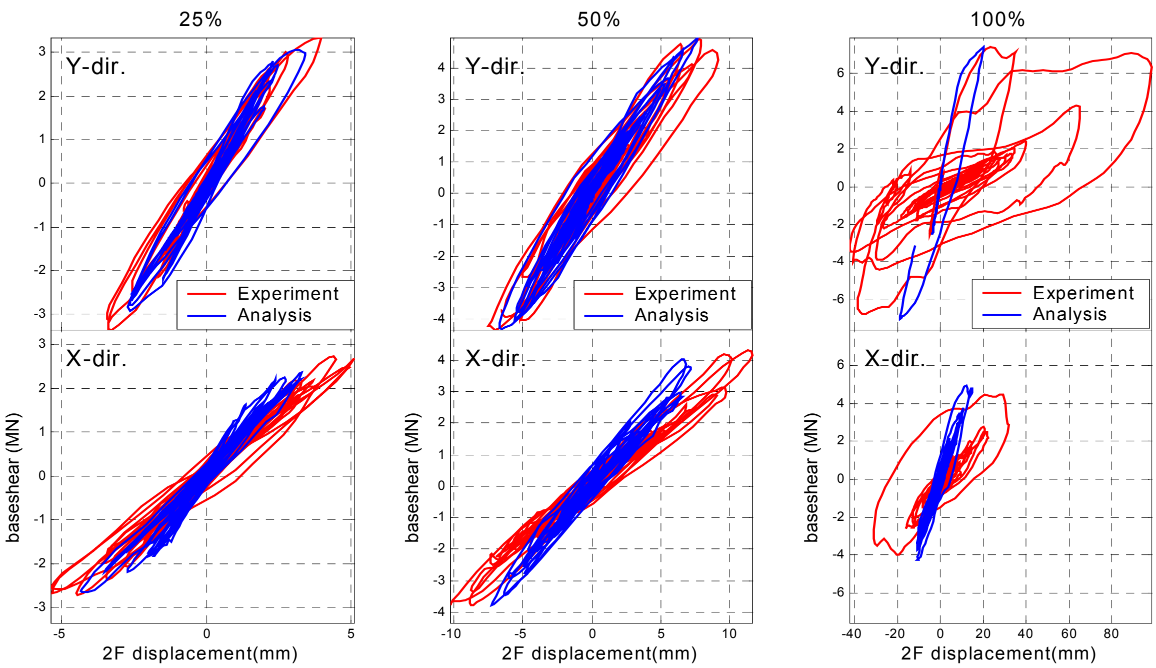

Figure 12 Relationship between base shear and 2F displacement (CASE2)

Figure 12 compares the test results to the analytical results obtained from modified model (CASE 2). It shows improved correlation between test and analysis as though displacement and base shear in analysis are still underestimated in X direction with wing wall frame. For maximum base shear, modified model agreed well with test results, but displacement discrepancy between test and analysis at INPUT-5 is still large (Figure 11 and 12). This poor agreement in displacement might arise from the fact that short columns and shear wall failed in shear and lost their lateral load resisting capacity inducing displacement concentration, but the analytical member model adopted in current analysis are not capable of simulating strength deterioration. In addition, the sliding between foundation and shake table is also major cause of the displacement discrepancy between test and analysis where the elastic springs were employed to simulate the support deformation.

5. SUMMARY

Maximum base shear obtained from CASE 1 model, whose evaluation for stiffness and strength was based on the equation commonly adopted in Japan, were underestimated throughout all loading stages. From the shear force distribution among frames, it is clear that shear force carried by columns is much smaller than that of test. Modified model (CASE 2) of which stiffness is a half of CASE 1 model and girder strength is recalculated by increasing the effective slab width showed a good correlation between test and analysis during INPUT-3 and 4. Maximum base shear during INPUT-5 could also be reproduced from the modified model (CASE 2) although the displacement discrepancy was still large, which was attributed to the inability of adopted member model in simulating strength deterioration and slip failure mode and the insufficient modeling for support condition.

REFERENCE

Kim, Y., and Kabeyasawa, T. (2005) Dynamic Analysis of Reinforced Concrete Wall-Frame to Collapse, *Proceedings of The First NEES/E-Defense Workshop on Collapse Simulation of Reinforced Concrete building Structures, Berkeley, USJ*, pp.181-194

Kim, Y., Kabeyasawa, T., Kabeyasawa, T., and Matsumori, T. (2007) Dynamic collapse analysis of the six-story full-scale wall-frame building，Proceedings of the 2007 Structures Congress, Long Beach, CA, USA, May 16-19

Matsumori, T., Shirai, K., and Kabeyasawa, T. (2006) Simulated Earthquake Test on a Full-Scale Six-Story Reinforced Concrete Building at E-Defense, Part 1: Outline of Test Program. *Proceedings of The Second NEES/E-Defense Workshop on Collapse Simulation of Reinforced Concrete building Structures, Miki Japan*,

Shirai, K., Matsumori, T., and Kabeyasawa, T. (2006) Simulated Earthquake Test on a Full-Scale Six-Story Reinforced Concrete Building at E-Defense, Part 2: Study on Distribution of Seismic Forces. *Proceedings of The Second NEES/E-Defense Workshop on Collapse Simulation of Reinforced Concrete building Structures, Miki Japan*.

Architectural Institute of Japan (1999). Design Guidelines for Earthquake Resistant Reinforced Concrete Buildings Base on Inelastic Displacement Concept, AIJ (in Japanese)

The Japan Building Disaster Prevention Association (2001), Standard for Seismic Evaluation of Existing Reinforced Concrete Buildings, The Japan Building Disaster Prevention Association (in Japanese)